

G.L. Myronchuk, V.P. Sachanyuk, O.V. Parasyuk, O.V. Zamurujeva

Phase Equilibria and Photoinduced Changes in the $\text{Ag}_2\text{S}-\text{In}_2\text{S}_3-\text{Si}(\text{Ge})\text{S}(\text{Se})_2$ Systems

Department of General and Inorganic Chemistry, Volyn State University, Voli Ave 13, 43025 Lutsk, Ukraine

The nature of equilibria in the $\text{Ag}_2\text{S}-\text{In}_2\text{S}_3-\text{Si}(\text{Ge})\text{S}_2$ systems was determined. The investigated vertical sections allow us to select the optimal conditions for the growth of the quaternary single crystals $\text{Ag}_2\text{In}_2\text{SiS}_6$ and $\text{Ag}_2\text{In}_2\text{GeS}_6$. Spectral distribution of the absorption coefficient and its photoinduced changes were studied. The possibility of using the investigated compounds as materials with controlled properties is demonstrated.

Key words: vertical sections, quasi-ternary system, disordered systems, photoinduced absorption.

Article acted received 12.11.2018; accepted for publication 15.12.2018.

Introduction

The study of the compound interaction in the I-III-X₂-IV-X₂ systems where I-Cu, Ag; III-Ga, In; IV-Si, Ge, Sn; X-S, Se are of interest due to the prospects of modifying the parameters of the ternary phases [1]. This makes possible their use in photovoltaics in the case of Cu-containing phases or non-linear optics which is typical of Ag-containing compounds. The formation of solid solution ranges of A^IC^{III}X₂ compounds and of quaternary compounds is characteristic of these systems. The most common of these are the phases 2-2-1-6 and 1-1-1-4. The mechanism of the solid solution formation consists of the gradual replacement of III atoms with Group IV elements in their crystallographic sites, whereas the sites of Group I atoms become vacancies [1]. The formation of the 2-2-1-6 compounds is more common for Ag-containing systems. They crystallize in two structures. The monoclinic structure (space group (SG) Cc) is typical of In compounds ($\text{Ag}_2\text{In}_2\text{Si}(\text{Ge})\text{S}_6$ [2], $\text{Ag}_2\text{In}_2\text{SiSe}_6$ [3], $\text{Ag}_2\text{In}_2\text{GeSe}_6$ [4]), whereas in cases where III is Ga the structure is the tetragonal SG I-42d ($\text{Ag}_2\text{Ga}_2\text{SiS}_6$ [5], $\text{Ag}_2\text{Ga}_2\text{SiSe}_6$ [6]). Only one compound of this composition is known in the copper-containing systems, but the $\text{Cu}_2\text{In}_2\text{SiS}_6$ compound (SG Cc) [7] is endothermic and exists in a fairly narrow temperature range 1107 – 1233 K. The 1-1-1-4 compounds form in both copper- and silver-based systems and are more diverse in structure. Two quaternary phases CuInSnS_4 and AgInSnS_4 have the spinel structure (SG $Fd\bar{3}m$) [8]. The orthorhombic SG Fdd2 is characteristic of the AgGaGeS_4 phase [9], while AgGaSiSe_4 crystallizes in SG Aea2 [10].

The structure acentricity of the chalcogenide crystals 2-2-1-6 is one of the reasons for their possible application as non-linear optical materials [2]. The isothermal sections of the $\text{Ag}_2\text{S}-\text{In}_2\text{S}_3-\text{Si}(\text{Ge})\text{S}_2$ systems at 300 K are presented in [7]. The $\text{Ag}_2\text{In}_2\text{Si}(\text{Ge})\text{S}_6$ are the only intermediate quaternary phases in the respective systems. However, the use of melt methods for the crystal growth of these phases requires information on the physico-chemical conditions of their formation obtainable from the phase diagrams involving the liquid which were not yet investigated.

The investigation of the spectral dependence of the absorption coefficient and photoconductivity of the $\text{Ag}_2\text{In}_2\text{SiS}(\text{Se})_6$ and $\text{Ag}_2\text{In}_2\text{GeS}(\text{Se})_6$ crystals was performed in [11, 12, 13]. The conductivity mechanism in various temperature ranges was determined, and the parameters of local levels in the band gap were calculated. Photoinduced absorption was studied to determine the possibilities of the most efficient use of these crystals in optoelectronic devices.

The objective of this work is to investigate vertical sections and liquidus surface projections (pertaining to the primary crystallization of the quaternary phases) of the $\text{Ag}_2\text{S}-\text{In}_2\text{S}_3-\text{Si}(\text{Ge})\text{S}_2$ systems which contain information for the single crystal growth conditions of the quaternary phases, and to study photoinduced absorption changes which can open up wide use in various optoelectronic devices such as optical triggers and switches.

I. Experimental

Phase equilibria in the $\text{Ag}_2\text{S}-\text{In}_2\text{S}_3-\text{SiS}_2$ and $\text{Ag}_2\text{S}-\text{In}_2\text{S}_3-\text{GeS}_2$ systems were investigated on 86 and 64 alloys, respectively. High-purity elements (at least 99.99 wt.%) were used as starting materials. Batches of 2 g mass were placed in quartz containers which were evacuated to the residual pressure of $\sim 10^{-2}$ Pa. The synthesis was performed by single-temperature method in a shaft-type furnace by gradual heating (at the rate of 10 K/h) to 1370 K with an intermediate stop at 820 K for

24 h. The maximum temperature was maintained for 3 h three hours, and cooling to room temperature was also at the rate of 10 K/h.

The alloys were investigated by differential-thermal method analysis for the vertical sections using a Paulik-Paulik-Erdey derivatograph, with Pt/Pt-Rh thermocouple. Al_2O_3 was used as a standard. The heating rate was 10 K/min, the cooling process was recorded in inertial mode.

Photoinduced absorption was studied using a solid-state laser at 980 nm wavelength. The absorption spectra

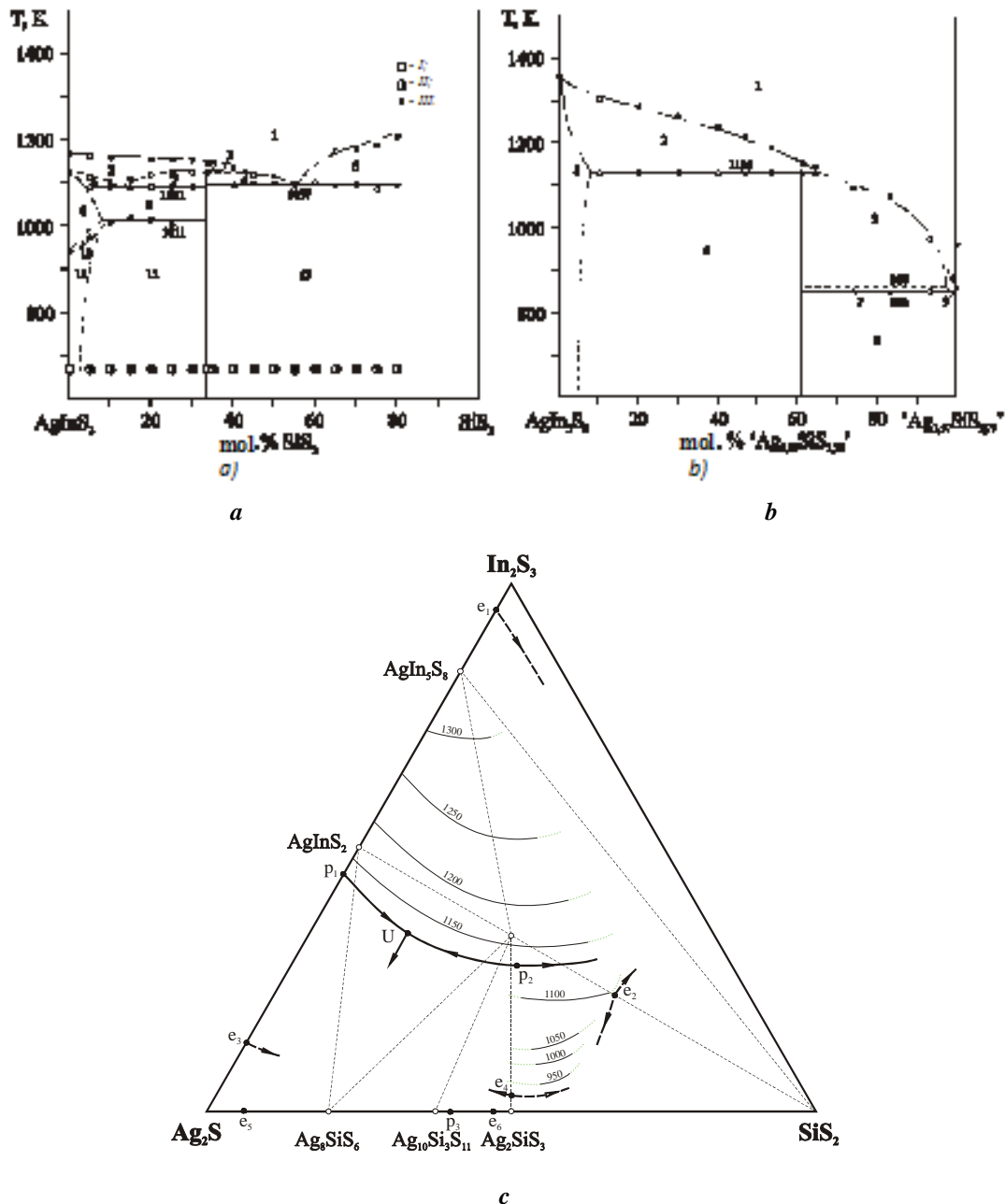


Fig. 1. Phase diagrams of the sections: a) $\text{AgInS}_2-\text{SiS}_2$: 1-L, 2-L+ AgIn_5S_8 , 3-L+ $\text{AgIn}_5\text{S}_8+\text{Ag}_2\text{In}_2\text{SiS}_6$, 4-L+ $\text{Ag}_2\text{In}_2\text{SiS}_6$, 5-L+ SiS_2 , 6-L+ $\text{AgIn}_5\text{S}_8+\alpha'$, 7-L+ $\text{AgIn}_5\text{S}_8+\text{Ag}_2\text{In}_2\text{SiS}_6$, 8- α' , 9- $\alpha'+\text{Ag}_2\text{In}_2\text{SiS}_6$, 10- $\alpha'+\alpha$, 11- α , 12- $\alpha+\text{Ag}_2\text{In}_2\text{SiS}_6$, 13- $\text{Ag}_2\text{In}_2\text{SiS}_6+\text{SiS}_2$; b) $\text{AgIn}_5\text{S}_8-\text{Ag}_{1.57}\text{Si}_{2.79}$: 1-L, 2-L+ ξ , 3-L+ $\text{Ag}_2\text{In}_2\text{SiS}_6$, 4-L+ Ag_2SiS_3 , 5- ξ , 6- $\xi+\text{Ag}_2\text{In}_2\text{SiS}_6$, 7-L+ $\text{Ag}_2\text{In}_2\text{SiS}_6+\text{Ag}_2\text{SiS}_3$, 8- $\text{Ag}_2\text{In}_2\text{SiS}_6+\text{Ag}_2\text{SiS}_3$, 9-L+ $\text{Ag}_2\text{SiS}_3+\text{SiS}_2$; I - single-phase alloys, II - two-phase alloys, III - DTA results; c) liquidus surface projection of the $\text{Ag}_2\text{S}-\text{In}_2\text{S}_3-\text{SiS}_2$ system in the region of the existence of $\text{Ag}_2\text{In}_2\text{SiS}_6$.

were recorded by an Ocean Optics optical spectrophotometer which monitors hyperfine absorption changes with an accuracy of 0.1 cm^{-1} . The photoinduced spectra were recorded before and during photostimulation.

II. Results and Discussion

Phase Diagrams

The AgInS_2 – SiS_2 section. The section was investigated in the range of 0–80 mol.% SiS_2 (Fig. 1 *a*). The liquidus consists of three curves of the primary crystallization of AgIn_5S_8 , $\text{Ag}_2\text{In}_2\text{SiS}_6$ and SiS_2 . The section is non-quasi-binary above the solidus due to the existence of the field of the primary crystallization of AgIn_5S_8 . The $\text{Ag}_2\text{In}_2\text{SiS}_6$ compound forms in the peritectic reaction $\text{L} + \text{AgIn}_5\text{S}_8 \leftrightarrow \text{Ag}_2\text{In}_2\text{SiS}_6$ at 1130 K with the component ratio 2:1. The horizontal line at

1091 K corresponds to the ternary peritectic process (U) of Fig. 1 (in), and the node at ~12.5 mol.% SiS_2 denotes the change of the secondary crystallization and separates binary peritectic processes. The interaction of $\text{Ag}_2\text{In}_2\text{SiS}_6$ and SiS_2 is eutectic, with the eutectic point coordinates of 57 mol.% SiS_2 and 1097 K. The homogeneity region of AgInS_2 at 670 K is < 5 mol.% SiS_2 . The polymorphism of AgInS_2 causes the peritectoid process $\alpha' + \text{Ag}_2\text{In}_2\text{SiS}_6 \leftrightarrow \alpha$ at 1011 K. The non-quasi-binarity of the sub-solidus part of the diagram disappears below 1091 and 1097 K where the intermediate quaternary phase is in equilibrium with α - AgInS_2 or SiS_2 .

The AgIn_5S_8 – $\text{Ag}_{1.57}\text{SiS}_{2.79}$ section. The formation of $\text{Ag}_2\text{In}_2\text{SiS}_6$ in the peritectic reaction $\text{L} + \text{AgIn}_5\text{S}_8 \leftrightarrow \text{Ag}_2\text{In}_2\text{SiS}_6$ at 1130 K was studied in detail in the phase diagram of the AgIn_5S_8 – $\text{Ag}_{1.57}\text{SiS}_{2.79}$ section (Fig. 1 *b*). The horizontal line at 850 K corresponds to the ternary eutectic, and the line at 860 K results from the binary eutectic interaction of $\text{Ag}_2\text{In}_2\text{SiS}_6$

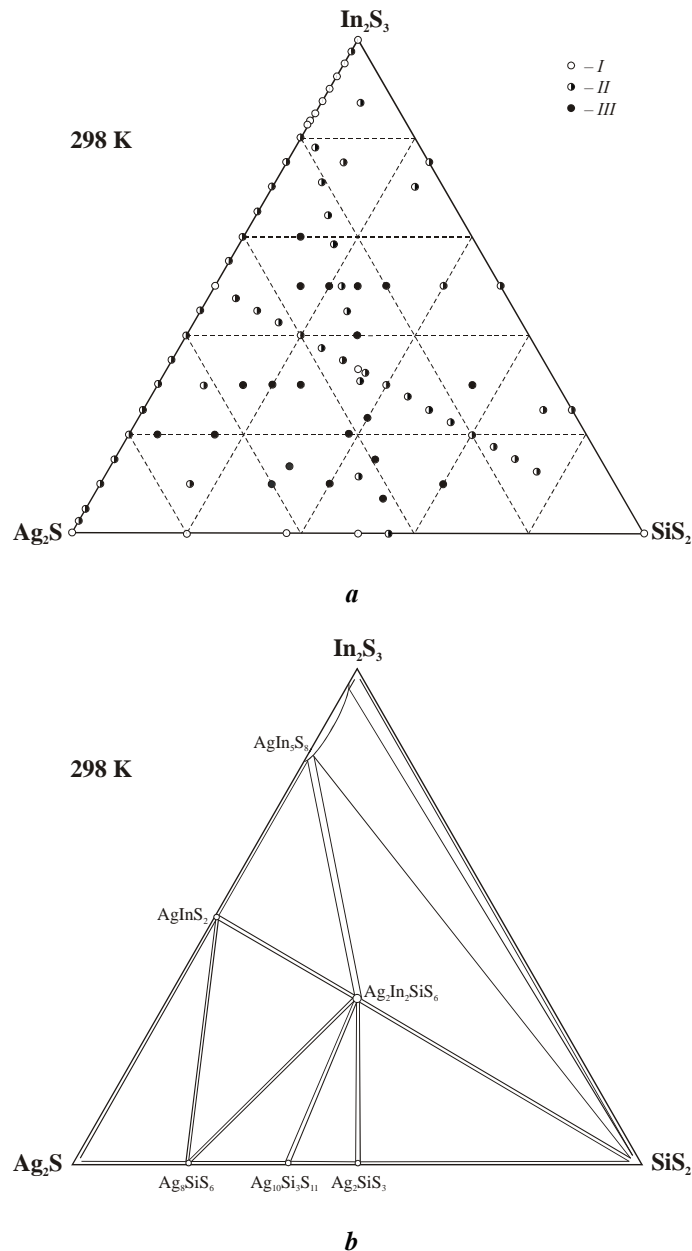


Fig. 2. Chemical and phase composition of alloys (*a*): (I - single-phase, II – two-phase, III – three-phase); and isothermal section of the Ag_2S – In_2S_3 – SiS_2 system at 298 K (*b*).

and Ag_2SiS_3 . Given the physico-chemical processes in the system, the section can be considered quasi-binary in the range of 0–61 mol.% ' $\text{Ag}_{1.57}\text{SiS}_{2.79}$ '. The sub-solidus region features binary equilibrium of AgIn_5S_8 and $\text{Ag}_2\text{In}_2\text{SiS}_6$ and the region of joint crystallization of $\text{Ag}_2\text{In}_2\text{SiS}_6$, Ag_2SiS_3 and SiS_2 .

Isothermal section of the $\text{Ag}_2\text{S}-\text{In}_2\text{S}_3-\text{SiS}_2$ system at 298 K. The chemical and phase composition of 86

alloys synthesized for the study of the interactions in this system is plotted in Fig. 2, *a*. The system is bounded by binary normal-valence sulfides of which polymorphous Ag_2S and In_2S_3 at room temperature are in LT modifications. The existence of five ternary compounds was confirmed at the study temperature (Fig. 2, *b*): LT- AgInS_2 (CuFeS_2 ST), AgIn_5S_8 (MgAl_2O_4 ST), LT- Ag_8SiS_6 (Ag_8GeS_6 ST), $\text{Ag}_{10}\text{Si}_3\text{S}_{11}$ ($\text{Ag}_{10}\text{Si}_3\text{S}_{11}$ ST),

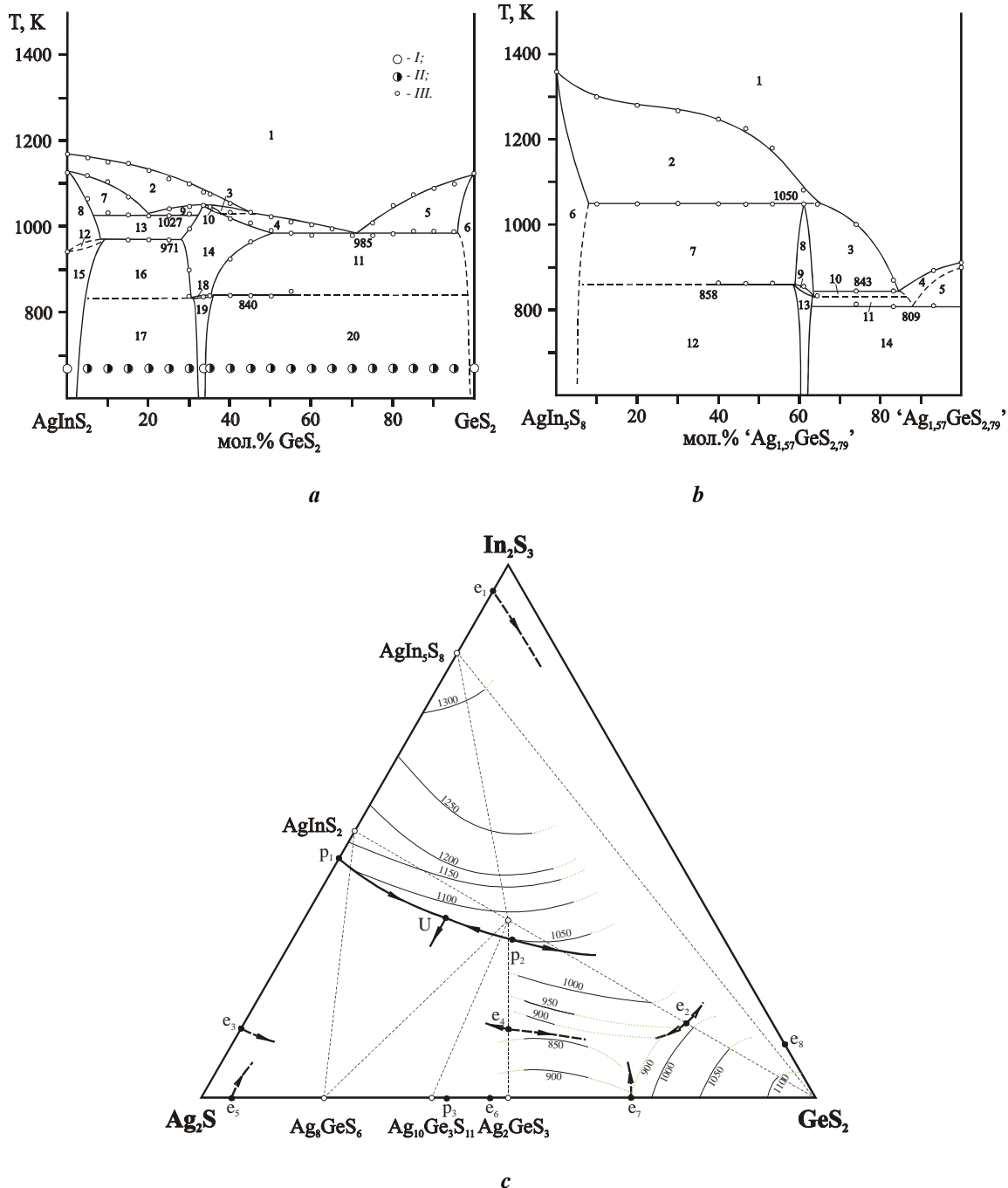


Fig. 3. Phase diagrams of the sections: *a*) $\text{AgInS}_2-\text{GeS}_2$: 1-L, 2-L+ AgIn_5S_8 , 3-L+ $\text{AgIn}_5\text{S}_8+\gamma'$, 4-L+ γ' , 5-L+ β , 6- β , 7-L+ $\text{AgIn}_5\text{S}_8+\alpha'$, 8- α' , 9-L+ $\text{AgIn}_5\text{S}_8+\gamma'$, 10- $\text{AgIn}_5\text{S}_8+\gamma'$, 11- $\gamma'+\beta$, 12- $\alpha+\alpha'$, 13- $\alpha'+\gamma'$, 14- γ' , 15- α , 16- $\alpha+\gamma'$, 17- $\alpha+\gamma'$, 18- $\gamma+\gamma'$, 19- γ , 20- $\gamma+\beta$; *b*) $\text{AgIn}_5\text{S}_8-\langle\text{Ag}_{1.57}\text{GeS}_{2.79}\rangle$ (6) 1-L, 2-L+ ξ , 3-L+ γ' , 4-L+ Ag_2GeS_3 , 5- $\text{Ag}_2\text{GeS}_3+\text{GeS}_2$, 6- ξ , 7- $\xi+\gamma'$, 8- γ' , 9- $\gamma'+\gamma$, 10-L+ $\gamma'+\text{Ag}_2\text{GeS}_3$, 11-L+ $\gamma+\text{Ag}_2\text{GeS}_3$, 12- $\xi+\gamma$, 13- γ , 14- $\gamma+\text{Ag}_2\text{GeS}_3+\text{GeS}_2$; I – single-phase alloys, II – two-phase alloys, III – DTA results; *c*) liquidus surface projection of the $\text{Ag}_2\text{S}-\text{In}_2\text{S}_3-\text{GeS}_2$ system in the vicinity of $\text{Ag}_2\text{In}_2\text{SiS}_6$.

Ag_2SiS_3 (Ag_2SiS_3 ST). The new quaternary compound $\text{Ag}_2\text{In}_2\text{SiS}_6$ has equilibria with all ternary sulfides and one binary, SiS_2 . The system features 16 quasi-binary equilibria of which 8 are triangulating sections thus forming 8 three-phase fields. Only the ternary spinel AgIn_5S_8 features a significant single-phase range. Other compounds do not form extended solid solutions. The maximum concentration range among the two-phase equilibria is occupied by the two-phase region $\text{AgIn}_5\text{S}_8+\text{SiS}_2$.

Liquidus surface projection of the $\text{Ag}_2\text{S}-\text{In}_2\text{S}_3-\text{SiS}_2$ system in the vicinity of $\text{Ag}_2\text{In}_2\text{SiS}_6$. Obtained results were used to plot in the first approximation a part of the liquidus surface projection of the system in the regions of the primary crystallization of AgIn_5S_8 and $\text{Ag}_2\text{In}_2\text{SiS}_6$ (Fig. 1, c). We suggest the existence of the peritectic reaction $\text{L}+\text{AgIn}_5\text{S}_8 \leftrightarrow \beta\text{-AgInS}_2+\text{Ag}_2\text{In}_2\text{SiS}_6$ at 1091 K. The monovariant lines originating from the binary peritectics p_1 and p_2 converge at the ternary peritectic point U. Due to its incongruent formation, the

region of the primary crystallization of $\text{Ag}_2\text{In}_2\text{SiS}_6$ is shifted from the stoichiometric composition towards lower In_2S_3 content. Microstructure analysis of the alloys in the concentration range between $\text{Ag}_2\text{In}_2\text{SiS}_6$ and Ag_2SiS_3 reveals eutectic nature of crystallization. Considering the stable equilibrium between these compounds, we conclude the formation of the binary eutectic of $\text{Ag}_2\text{In}_2\text{SiS}_6$ and Ag_2SiS_3 . The monovariant lines originating from the point e_4 to both sides of it will show a decrease in temperature according to the Van Rijn rule. The position of the point e_4 is shifted to Ag_2SiS_3 (at the $\text{Ag}_2\text{In}_2\text{SiS}_6-\text{Ag}_2\text{SiS}_3$ section) as can be seen from the $\text{AgIn}_5\text{S}_8-\text{Ag}_{1.57}\text{SiS}_{2.79}$ section. The region of the primary crystallization of $\text{Ag}_2\text{In}_2\text{SiS}_6$ features significant temperature decreases and is promising for the selection of the starting compositions for the growth of its single crystals.

The $\text{Ag}_2\text{S}-\text{In}_2\text{S}_3-\text{GeS}_2$ system. Vertical section $\text{AgInS}_2-\text{GeS}_2$. The phase diagram of the $\text{AgInS}_2-\text{GeS}_2$ section is shown in Fig. 3, a. Due to the peritectic

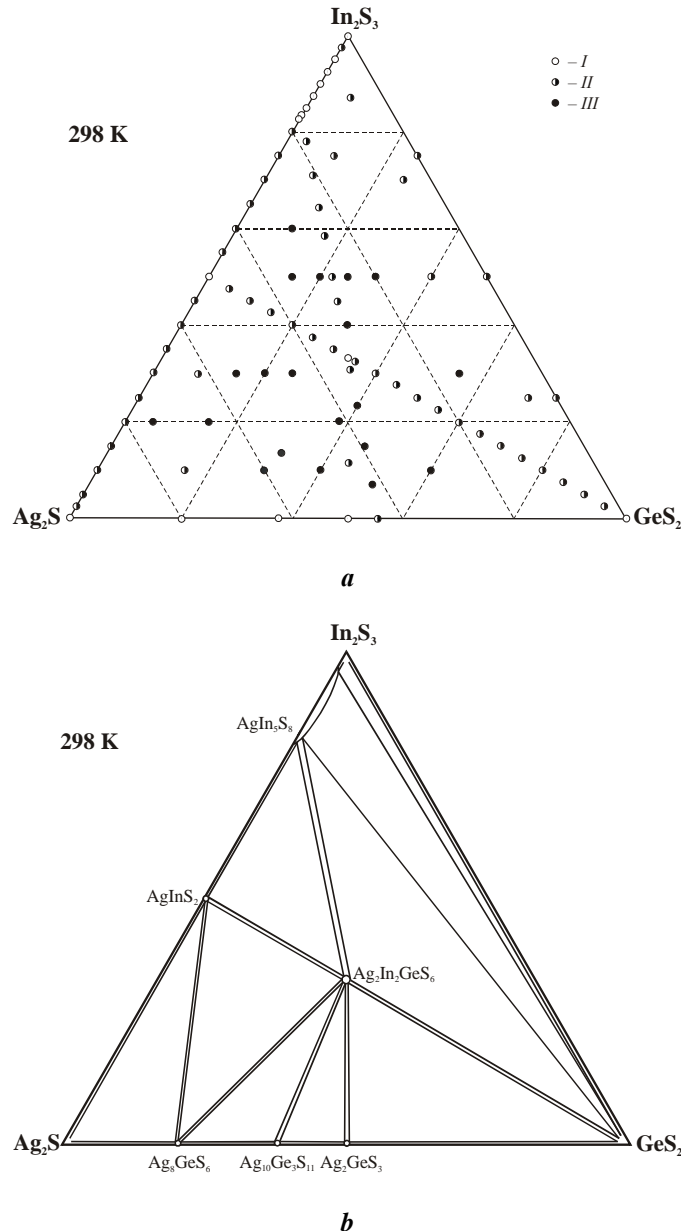


Fig. 4. Chemical and phase composition of alloys (a) (I – single-phase alloys, II – two-phase alloys, III – three-phase alloys); and isothermal section of the $\text{Ag}_2\text{S}-\text{In}_2\text{S}_3-\text{GeS}_2$ system at 298 K (b).

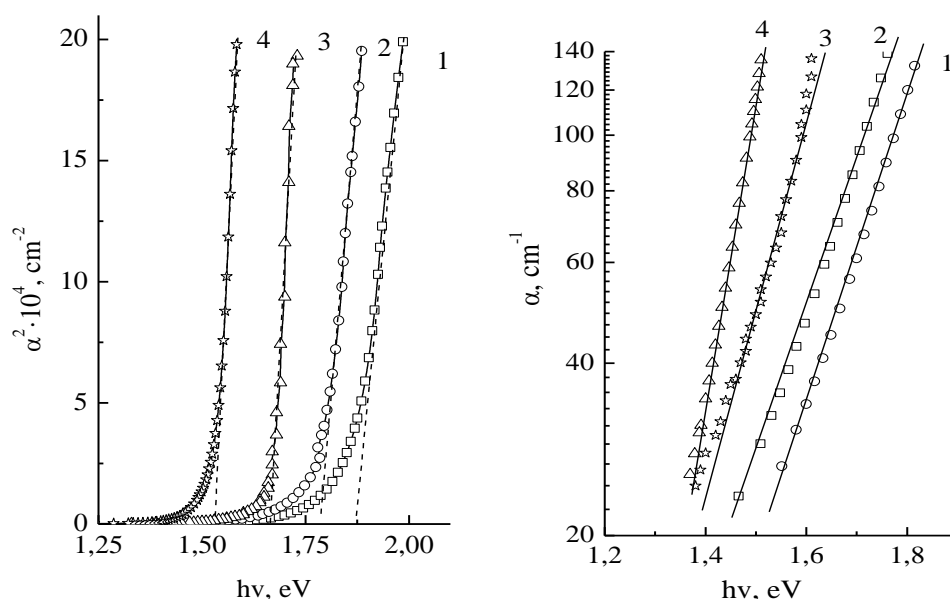


Fig. 5. Spectral distribution of the absorption coefficient at 300 K (left); bandgap energy estimate $\ln \alpha = f(h\nu)$ for compounds: 1. $\text{Ag}_2\text{In}_2\text{SiS}_6$; 2. $\text{Ag}_2\text{In}_2\text{GeS}_6$; 3. $\text{Ag}_2\text{In}_2\text{SiSe}_6$; 4. $\text{Ag}_2\text{In}_2\text{GeSe}_6$.

Table 1

Estimated bandgap energy, Urbach's rule parameters and the parameters of the electron-phonon interaction

Crystal	E_g , eV	E_u , eV	n_t , 10^{17} cm^{-3}	σ_0 , arb.u	$h\nu_0$, (± 1.0) eV	g
$\text{Ag}_2\text{In}_2\text{SiS}_6$	1.88	0.14	12.34	0.54	0.15	1.23
$\text{Ag}_2\text{In}_2\text{GeS}_6$	1.81	0.15	13.23	0.5	0.15	1.33
$\text{Ag}_2\text{In}_2\text{SiSe}_6$	1.67	0.13	11.46	0.54	0.14	1.23
$\text{Ag}_2\text{In}_2\text{GeSe}_6$	1.54	0.11	9.70	0.55	0.12	1.21

formation of AgInS_2 , the investigated system is non-quasi-binary in the range of 0 - 47 mol% GeS_2 . The section liquidus consists of three curves of the primary crystallization of AgIn_5S_8 , $\beta\text{-Ag}_2\text{In}_2\text{GeS}_6$ and GeS_2 . The solidus consists of two horizontal lines at 1027 and 985 K and four curves that bound the homogeneity regions of the end components and the intermediate compound.

The polymorphous transformation of AgInS_2 is the reason for the peritectoid decomposition of α' at 970 K. The homogeneity region of $\text{Ag}_2\text{In}_2\text{GeS}_6$ at annealing temperature 670 K ranges within 32 - 35 mol.% GeS_2 . According to XRD results, all alloys in this region crystallize in the monoclinic structure. As the intermediate quaternary phase is dimorphous, the thermograms feature endothermic effects that reach the maximum value at the stoichiometric composition. The phase transformation in the AgInS_2 -enriched region occurs at 833 K, and 840 K at the GeS_2 -rich side. The quaternary phase forms a eutectic with GeS_2 with coordinates of 73 mol.% GeS_2 and 985 K. According to [3], GeS_2 is dimorphous, but no thermograms record an effect corresponding to its polymorphous transformation. The solid solubility based on GeS_2 is <2 mol. % AgInS_2 at 670 K.

The $\text{AgIn}_5\text{S}_8-\text{Ag}_{1.57}\text{GeS}_{2.79}$ section. The phase diagram of the $\text{AgIn}_5\text{S}_8-\text{Ag}_{1.57}\text{GeS}_{2.79}$ section (Fig. 3, b)

was investigated to clarify the interaction in the $\text{AgInS}_2-\text{GeS}_2$ system. The intermediate compound $\text{Ag}_2\text{In}_2\text{GeS}_6$ forms in the peritectic reaction $L+\text{AgIn}_5\text{S}_8\rightleftharpoons\text{Ag}_2\text{In}_2\text{GeS}_6$. The polymorphous modification of the intermediate phase results in the appearance of the horizontal line in the sub-solidus part at 855 K in the $\text{AgIn}_5\text{S}_8-\text{Ag}_2\text{In}_2\text{GeS}_6$ region and at 830 K at the right side of the diagram. Microstructure analysis of the alloys in the of 61 - 100 mol.% ' $\text{Ag}_{1.57}\text{GeS}_{2.79}$ ' range reflects the eutectic nature of crystallization, so the horizontal line at 809 K corresponds to the ternary eutectic process.

Isothermal section of the $\text{Ag}_2\text{S}-\text{In}_2\text{S}_3-\text{GeS}_2$ system at 298 K. The interactions in the quasi-ternary system $\text{Ag}_2\text{S}-\text{In}_2\text{S}_3-\text{GeS}_2$ were studied on 90 samples (Fig. 4, a). Five ternary compounds exist in the side systems: AgInS_2 , AgIn_5S_8 , $\text{LT-Ag}_8\text{GeS}_6$ (Ag_8GeS_6 ST), $\text{Ag}_{10}\text{Ge}_3\text{S}_{11}$ ($\text{Ag}_{10}\text{Ge}_3\text{S}_{11}$ ST), Ag_2GeS_3 (Ag_2SiS_3 ST). The system is formed by binary sulfides that are characterized by polymorphism. The quaternary compound $\text{Ag}_2\text{In}_2\text{GeS}_6$ that forms in the system has at 298 K binary equilibria with all ternary sulfides and with one binary, GeS_2 (Fig. 4, b). There are 8 triangulating sections in the system which separate 8 three-phase fields. Only the AgIn_5S_8 phase has a notable homogeneity region.

Liquidus surface projection of the $\text{Ag}_2\text{S}-\text{In}_2\text{S}_3-\text{GeS}_2$ system in the field of the primary crystallization

of $\text{Ag}_2\text{In}_2\text{GeS}_6$. Liquidus surface projection of the quaternary system in the vicinity of the primary crystallization of AgIn_5S_8 and $\beta\text{-Ag}_2\text{In}_2\text{GeS}_6$ was constructed from this study and literature data [4] (Fig. 3, c). The system features the ternary peritectic reaction $L + \text{AgIn}_5\text{S}_8 \leftrightarrow \alpha' + \gamma'$ at 1050 K. The monovariant lines originating from the binary peritectics p_1 and p_2 converge to point U.

Due to the incongruous type of formation, the region of the primary crystallization of $\beta\text{-Ag}_2\text{In}_2\text{GeS}_6$ is shifted from the stoichiometric composition towards the lower In_2S_3 content. Microstructure analysis of the alloys lying between $\text{Ag}_2\text{In}_2\text{GeS}_6$ and Ag_2GeS_3 reveals eutectic type of crystallization. Considering the stable equilibrium between these compounds, the formation of the binary eutectic of $\text{Ag}_2\text{In}_2\text{SiS}_6$ and Ag_2SiS_3 is concluded. Both monovariant lines originating from the point e_4 should show temperature decrease according to the Van Rijn rule. The point e_4 is shifted to Ag_2GeS_3 at the $\text{Ag}_2\text{In}_2\text{GeS}_6\text{-Ag}_2\text{GeS}_3$ section (see the $\text{AgIn}_5\text{S}_8\text{-Ag}_{1.57}\text{GeS}_{2.79}$ section). The determination of the field of the primary crystallization of the quaternary phase is an important element in the study of phase equilibria since the initial compositions for the single crystal growth using solution-melt methods is chosen from such concentration range.

III. Photoinduced optical properties

The position and shape of the fundamental absorption edge is one of the principal factors determining the optical properties of the $\text{AgInSe}_2\text{-Si(Ge)S(Se)}_2$ crystals. Therefore, we studied the spectra of optical absorption of these compounds. The absorption coefficient was calculated from the recorded transmission spectra using the formula taking into account multiple internal reflections in a parallel-plane

sample [14]:

$$\alpha = \frac{1}{d} \ln \left\{ \frac{(1-R)^2}{2T} + \sqrt{\left[\frac{(1-R)^2}{2T} \right]^2 + R^2} \right\},$$

where α is the absorption coefficient, d is the sample thickness, T is transmission, R is the reflection coefficient.

Since the ternary compounds $\text{A}^{\text{III}}\text{B}^{\text{III}}\text{C}^{\text{VI}}$ are materials with direct interband transitions [13], the bandgap energy E_g was estimated by extrapolating the linear region of the dependence of α^2 on the photon energy to the intersection with the abscissa (Fig. 5).

The closeness of E_g values for various $\text{AgInSe}_2\text{-Si(Ge)S(Se)}_2$ crystals (Table 1) shows that the bandgap energy of the quaternary chalcogenide is determined by the nature of the chalcogen atoms (S, Se) and Ag and In cations the concentration of which in the compounds is higher compared to Si or Ge atoms.

According to [13], the shape of the optical absorption edge remains exponential for the investigated compounds in the temperature range 100 – 300 K, and Urbach's energy does not change with temperature (Table 1). The adherence to Urbach's rule and large E_U values mean that the $\text{Ag}_2\text{In}_2\text{Si(Ge)S}_6$ and $\text{Ag}_2\text{In}_2\text{Si(Ge)Se}_6$ crystals are defect semiconductors whose electronic structure approaches that of disordered systems [15]. According to Urbach's method [16], the slope parameter was determined that is approximated in the studied temperature range by the expression for the absorption edge, which is formed with the participation of electron-phonon interaction [17, 18]. The calculated parameters are given in Table 1. The constant g of the electron/exciton-phonon interaction is greater than 1 which is typical of crystals with non-stoichiometry defects in cation sub-lattice [19]. This is in good agreement with the data of [12, 13].

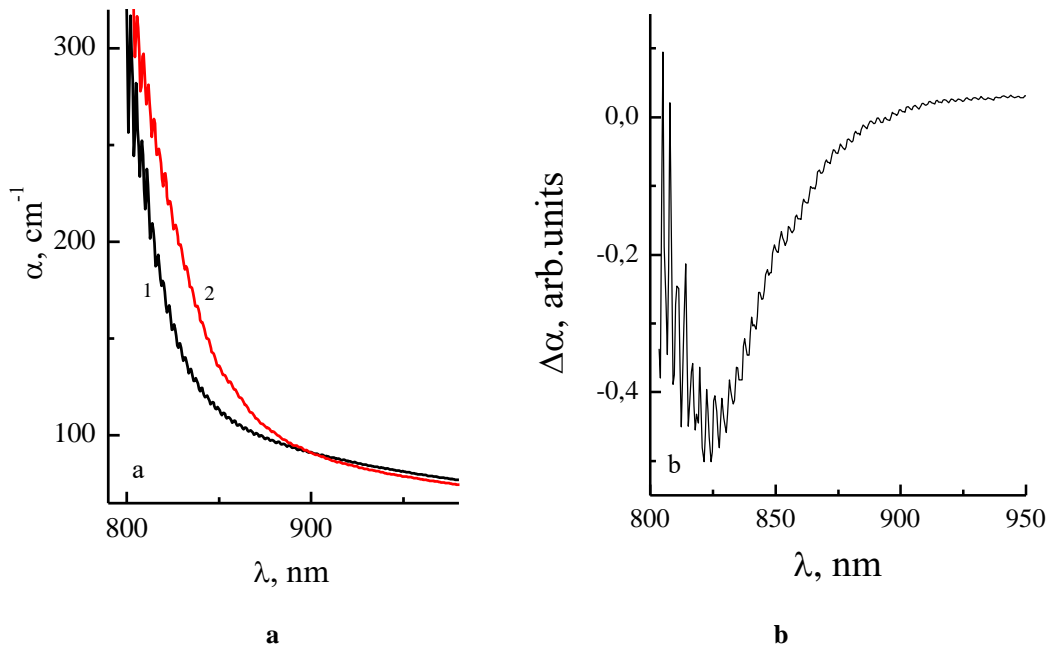


Fig. 6. a) Spectral dependence of the absorption coefficient: 1) prior to irradiation; 2) after 1 min irradiation with a 980 nm laser; b) change in the absorption coefficient.

Photoinduced changes in the absorption coefficient were studied to discover the most effective use of $\text{AgInSe}_2-\text{Si}(\text{Ge})\text{Se}_2$ compounds in optoelectronic devices. The slope of Urbach's tail becomes less steep upon illumination (Fig. 6) indicating additional absorption which is due either to increased concentration of defects with energy levels in the band gap or to the appearance of internal electric field from the creation of charged defects. The absorption decreases at higher energies because the total number of metastable states cannot be changed by the illumination. Therefore an increase in absorption in one energy region leads to a decrease in another region.

Therefore, the change in photoinduced absorption under laser irradiation that excites the electronic subsystem occurs not due to the shift of the fundamental absorption edge but due to the change in the occupation of the intrinsic defect subsystem under photoinduced excitation.

Photoinduced changes under irradiation with CO_2 laser and with a 980 nm laser are similar [20], i.e., the changes occur in the region near the absorption edge, and red spectral shift is observed with increased irradiation time. This can be explained by the domination of the same mechanism for two types of excitations, namely, significant electron-phonon interaction. When irradiated with a 980 nm laser, photoinduced changes are associated with pure electronic transitions which include trap levels of electronic origin within the band gap close to the fundamental absorption edge. When irradiated with CO_2 laser, these levels are excited as a result of the phonon interaction. The similarity of the changes induced by a solid-state laser at 980 nm and CO_2 laser

[20] shows the fundamental role of the electron-phonon interaction. The study of the change of the absorption coefficient near the fundamental absorption edge induced by the solid-state laser shows the absence of irreversible modifications. This allows the use of these materials as optically controlled materials for visible and infrared lasers.

Conclusions

Phase equilibria in the $\text{Ag}_2\text{S}-\text{In}_2\text{S}_3-\text{Si}(\text{Ge})\text{S}_2$ systems were characterized. Vertical sections were investigated to select the conditions for the single crystal growth of the novel non-centrosymmetric quaternary chalcogenides $\text{Ag}_2\text{In}_2\text{SiS}_6$ and $\text{Ag}_2\text{In}_2\text{GeS}_6$. Their bandgap energy was estimated from the study of the spectral distribution of the absorption coefficient of the $\text{AgInSe}_2-\text{Si}(\text{Ge})\text{S}(\text{Se})_2$ crystals. Investigation of the optical properties of selenide compounds in comparison with sulfides shows that the bandgap energy decreases under $\text{S} \Rightarrow \text{Se}$ substitution. Photoinduced changes in the absorption coefficient under the influence of the solid-state laser with 980 nm wavelength were observed.

Myronchuk G.L. - Ph.D., Associate Professor of the Department of Experimental Physics and Information and Measurement Technologies;

Sachanyuk V.P. - Researcher;

Parasyuk O.V. - Ph.D., Professor, Dean of the Faculty of Chemistry;

Zamurujeva O.V. - Ph.D., senior researcher.

- [1] V. P. Sachanyuk, Phase equilibrium and phase properties in quasi-triple systems formed by chalcogenides of elements of 3d - and Ib, IIb, IIIb, IVa, b subgroups (Author's abstract, Candidate of Chemical Science, Lviv, 2008).
- [2] V. P. Sachanyuk, G. P. Gorgut, V. V. Atuchin, I. D. Olekseyuk, O. V. Parasyuk, J. Alloys Comp. 452, 348 (2008) (doi:10.1016/j.jallcom.2006.11.043).
- [3] I. D. Olekseyuk, V. P. Sachanyuk, O. V. Parasyuk, J. Alloys Comp. 414(1-2), 73 (2006) (doi:10.1016/j.jallcom.2005.07.025).
- [4] O.V. Krykhovets, L.V. Sysa, I.D. Olekseyuk, T. Glowiyak, J. Alloys Compds. 287, 181 (1999) (doi:10.1016/S0925-8388(99)00016-X).
- [5] M. Piasecki, G.L. Myronchuk, O.V. Parasyuk and other J. Sol. State Chem. 246, 363 (2017) (doi:10.1016/j.jssc.2016.12.011).
- [6] O. V. Parasyuk, V. V. Pavlyuk, O. Y. Khyzhun, RSC Advances 6, 90958 (2016) (doi:10.1039/C6RA19558J).
- [7] V. P. Sachanyuk, I. D. Olekseyuk, O. V. Parasyuk, J. Alloys Comp. 443(1-2), 61 (2007) (doi:10.1016/j.jallcom.2006.09.131).
- [8] I.D. Olekseyuk, G.P. Gorgut, M.V. Shevchuk, Polish J. Chem. 76 915 (2002).
- [9] O.Y. Khyzhun, O.V. Parasyuk, A.O. Fedorchuk, Advances in Alloys and Compounds 1(1), 15 (2014).
- [10] S. Zhang, D. Mei, X.Du, and other, J. Sol. State Chem. 238, 21 (2016).
- [11] M. Chmiel, M. Piasecki, G. Myronchuk, G. Lakshminarayana, A. H. Reshak, O. G. Parasyuk, Yu. Kogut, I. V. Kityk., Spectrochim Acta A 91:48, (2012) (doi:10.1016/j.saa.2012.01.053).
- [12] O. V. Zamurujeva, G. L. Myronchuk, M. V. Khvyshchun, O. V. Parasyuk, Physics and Chemistry of Solid State 17(2), 202 (2016) (doi:10.15330/pcss.17.2.202-206).
- [13] M. Makowska-Janusik, I. V. Kityk, G. Myronchuk, Cryst. Eng. Comm. 16, 9534 (2014) (doi:10.1039/C4CE01005A).
- [14] O.V. Krykhovets, L.V. Sysa, I.D. Olekseyuk, T. Glowiyak, J. Alloys Compds. 287, 181 (1999) (doi:10.1016/S0925-8388(99)00016-X).

- [15] M. Chmiel, M. Piasecki, G. Myronchuk, G. Lakshminarayana, and other, Spectrochimica Acta Part A 91, 48 (2012) (doi:10.1016/j.saa.2012.01.053).
- [16] N. Mott, Electronic processes in non-crystalline substances. 2nd ed. (M.: Mir, 1982).
- [17] L. Stilbans Physics of semiconductors (M.: Sov. Radio, 1967).
- [18] M. V. Kurik, Maik, Fiz. Tverd. Tela 33, 615 (1991).
- [19] M.V.Kurik, Wiley-VCH, Phys. Stat. Sol. 8(a), 9 (1971) (doi:10.1002/pssa.2210080102).
- [20] T. Panchenko, S. Kopylova, Yu. Osetskii, Physics of the Solid State 37 1415 (1995).
- [21] E. Al-Harbi, A. Wojciechowski, N. AlZayed, O.V. Parasyuk, E. Gondek, P. Armatys, A.M. El-Naggar, I.V. Kityk, P. Karasinski Spectrochimica Acta Part A: Molecular and Biomolecular Spectroscopy 111 142 (2013) (doi:10.1016/j.saa.2013.03.054).

Г.Л. Мирончук, В.П. Сачанюк, О.В. Парасюк, О.В. Замуруєва

Фазові рівноваги та фотоіндуковані зміни у системах $\text{Ag}_2\text{S-In}_2\text{S}_3\text{-Si(Ge)S(Se)}_2$

*Східноєвропейський національний технічний університет імені Лесі Українки, просп. Волі, 13, Луцьк,
43025, Україна, e-mail:zamuraeva.o@gmail.com*

У роботі встановлений характер рівноваг у системах $\text{Ag}_2\text{S-In}_2\text{S}_3\text{-Si(Ge)S}_2$ та досліджені політермічні перетини дозволяють вибрати оптимальні умови росту монокристалів тетраарних халькогенідів $\text{Ag}_2\text{In}_2\text{SiS}_6$ і $\text{Ag}_2\text{In}_2\text{GeS}_6$. Проведено дослідження спектрального розподілу коефіцієнта поглинання та його фотоіндукованих змін. Показано можливість використання досліджуваних сполук в якості матеріалів з керованими властивостями.

Ключові слова: політермічні перетини, квазіпотрійна система, неупорядковані системи, фотоіндуковане поглинання.